

Analyst

Accepted Manuscript



This is an *Accepted Manuscript*, which has been through the Royal Society of Chemistry peer review process and has been accepted for publication.

Accepted Manuscripts are published online shortly after acceptance, before technical editing, formatting and proof reading. Using this free service, authors can make their results available to the community, in citable form, before we publish the edited article. We will replace this *Accepted Manuscript* with the edited and formatted *Advance Article* as soon as it is available.

You can find more information about *Accepted Manuscripts* in the [Information for Authors](#).

Please note that technical editing may introduce minor changes to the text and/or graphics, which may alter content. The journal's standard [Terms & Conditions](#) and the [Ethical guidelines](#) still apply. In no event shall the Royal Society of Chemistry be held responsible for any errors or omissions in this *Accepted Manuscript* or any consequences arising from the use of any information it contains.

1
2
3 **Microchip Electrophoresis with Amperometric Detection Method for Profiling**
4
5 **Cellular Nitrosative Stress Markers**
6
7
8
9

10 Dulan B. Gunasekara,^{1,2} Joseph M. Siegel,^{1,2} Giuseppe Caruso,^{1,3}

11
12 Matthew K. Hulvey,^{1,4} Susan M. Lunte^{1,2,5}
13
14
15

16
17 ¹Ralph N. Adams Institute for Bioanalytical Chemistry, University of Kansas, Lawrence,
18 KS, USA
19

20
21 ²Department of Chemistry, University of Kansas, Lawrence, KS, USA
22

23 ³Department of Chemical Science, Section of Biochemistry and Molecular Biology,
24 University of Catania, Italy
25

26
27 ⁴Akermin, Inc., St. Louis, MO, USA
28

29 ⁵Department of Pharmaceutical Chemistry, University of Kansas, Lawrence, KS, USA
30
31
32

33
34 Correspondence:
35

36 Professor Susan M. Lunte,
37

38 Ralph N. Adams Institute for Bioanalytical Chemistry, University of Kansas
39

40 2030 Becker Drive, Lawrence, KS 66047 USA
41

42
43 E-mail: slunte@ku.edu
44

45
46 Phone: +1-785-864-3811
47

48 Fax: +1-785-864-1916
49
50
51
52
53
54
55
56
57
58
59
60

Summary

The overproduction of nitric oxide (NO) in cells results in nitrosative stress due to the generation of highly reactive species such as peroxynitrite and N_2O_3 . These species disrupt the cellular redox processes through the oxidation, nitration, and nitrosylation of important biomolecules. Microchip electrophoresis (ME) is a fast separation method that can be used to profile cellular nitrosative stress through the separation of NO and nitrite from other redox-active intracellular components such as cellular antioxidants. This paper describes a ME method with electrochemical detection (ME-EC) for the separation of intracellular nitrosative stress markers in macrophage cells. The separation of nitrite, azide (interference), iodide (internal standard), tyrosine, glutathione, and hydrogen peroxide (neutral marker) was achieved in under 40 s using a run buffer consisting of 7.5 to 10 mM NaCl, 10 mM boric acid, and 2 mM TTAC at pH 10.3 to 10.7. Initially, NO production was monitored by the detection of nitrite (NO_2^-) in cell lysates. There was a 2.5- to 4-fold increase in NO_2^- production in lipopolysaccharide (LPS)-stimulated cells. The concentration of NO_2^- inside a single unstimulated macrophage cell was estimated to be 1.41 mM using the method of standard additions. ME-EC was then used for the direct detection of NO and glutathione in stimulated and native macrophage cell lysates. NO was identified in these studies based on its migration time and rapid degradation kinetics. The intracellular levels of glutathione in native and stimulated macrophages were also compared, and no significant difference was observed between the two conditions.

1. Introduction

NO is involved in several important physiological processes, including neurotransmission, regulation of blood flow, platelet aggregation, and inactivation of pathogens and bacteria.^{1, 2} NO is produced in cells through the activation of nitric oxide synthase (NOS) and the conversion of L-arginine into L-citrulline.^{1, 2} There are three isoforms of NOS; namely neuronal, endothelial, and inducible NOS. Activation of inducible NOS (iNOS) is a part of the immune response and leads to the production of large amounts of NO over a long period of time. These elevated NO concentrations can be harmful due to the formation of reactive nitrogen species such as N_2O_3 and peroxynitrite.^{1, 2} Both of these species are highly reactive and capable of participating in oxidative stress and nitration/nitrosylation of important biomolecules *in vivo*.³⁻⁵

There are many different types of immune cells in the human body, and macrophages are the primary cell type that is activated as part of an immune response.^{2, 6} It is also well known that monocytes can be differentiated into macrophages, and it has been shown that monocytes in blood can migrate into the intima of a blood vessel and can be differentiated into macrophages during atherosclerosis.^{7, 8} Macrophages produce NO primarily through the activation of iNOS; however, an uncontrolled or large NO production in these cell types results in cellular nitrosative stress, which has been implicated in many neurodegenerative and cardiovascular diseases.^{1, 9} The toxic effects of cellular pro-oxidants produced from NO can be mitigated by the presence of antioxidant molecules in the cell.^{10, 11} Glutathione (GSH) is an antioxidant produced by the cells that can scavenge NO and produce nitrosoglutathione. Also, GSH can react with hydrogen peroxide to form glutathione

1
2
3 disulfide. This reaction is catalyzed in the cell by glutathione peroxidase.^{10, 11} The
4
5 balance between pro- and antioxidants is important for regulating cellular nitrosative
6
7 stress.¹²
8
9

10
11 There is a wide range of methods reported for the direct and indirect detection of
12
13 NO. The Griess assay is used extensively for the detection of NO based on a
14
15 colorimetric reaction with a NO metabolite (NO_2^-) due to its simplicity. Other analytical
16
17 methods that have been used for the determination of NO are UV-visible spectroscopy,
18
19 electron paramagnetic resonance spectroscopy, chemiluminescence, amperometry,
20
21 and voltammetry.¹³⁻¹⁷ NO can be directly detected by amperometric detection, and NO
22
23 biosensors are commonly used in biological applications.¹⁶⁻¹⁸ However, despite their low
24
25 limits of detection (LOD), biosensors can suffer from the presence of interferences and
26
27 also lack the ability to detect multiple analytes simultaneously.
28
29
30

31
32 Another popular approach for NO detection is the use of fluorescent probes such
33
34 as diaminofluorofluorescein diacetate (DAF-FM DA, specific for NO) and
35
36 diaminonaphthalene (specific for NO_2^-).¹⁹ However, these probes can cross-react with
37
38 other species in the sample. Also, microscopic imaging or common spectrometry-based
39
40 methods cannot distinguish the signal of the desired analyte from those of
41
42 interferences.¹⁹⁻²¹ Interferences can be avoided by separating them from the analyte of
43
44 interest; and therefore, separation-based approaches such as liquid chromatography
45
46 (LC) and capillary electrophoresis (CE) have become popular for the determination of
47
48 NO.^{15, 21}
49
50
51

52
53 CE has many advantages over liquid chromatographic methods, including very low
54
55 sample volume requirements, higher separation efficiencies, and faster separations.
56
57
58
59
60

1
2
3 Therefore, CE has been used for detection of NO from various biological samples.²²⁻²⁶
4
5 CE with laser-induced fluorescence (LIF) detection has been extensively used for direct
6
7
8 monitoring of NO using selective fluorescent probes.^{21, 26} Conductivity and UV detection
9
10 have also been employed with CE for the indirect detection of NO by monitoring its
11
12 degradation products, nitrite and nitrate.^{22-25, 27}
13
14

15 More recently, microfluidic devices have been employed to detect the production of
16
17 cellular NO and its metabolites.²⁸⁻³³ These devices have many advantages over
18
19 classical methods for the study of NO, including the possibility of performing on-chip cell
20
21 culture, simulating the cellular response in constricted blood vessels, modeling *in vivo*
22
23 environments by immobilizing cells on a microchannel, and single cell analysis that can
24
25 be difficult to achieve using classical methods.²⁸⁻³³ Spectroscopic detection is
26
27 predominantly used in these devices, and methods for monitoring NO production from
28
29 erythrocytes,³³ endothelial,³⁴ and macrophage cells³¹ have been reported. Separations
30
31 with microfluidic devices are most commonly performed using electrophoresis. The use
32
33 of high field strengths with short channels in the planar format makes it possible to
34
35 routinely perform subminute separations using this technique. Therefore, this method is
36
37 especially useful for the detection of chemically labile species since they can be
38
39 separated and detected before significant degradation occurs.³⁵
40
41
42
43
44
45

46 Recently, we reported a method for the determination of intracellular NO production
47
48 in cell lysates using DAF-FM and ME-LIF.³⁶ This method was limited to the
49
50 determination of NO and could not be used to detect any other RNOS related species.
51
52 NO can also be detected by amperometric detection, and we also recently reported a
53
54 ME-EC method for the detection of NO and NO₂⁻ produced by NONOate salts.³⁵ Since
55
56
57
58
59
60

1
2
3 nitrate (NO_3^-) is not electroactive, a method using an on-chip Cu^{2+}/Cd reductor can be
4 used to reduce NO_3^- to NO_2^- , which permits the detection of both species by ME-EC.³⁷
5
6 Nitrate and nitrite can also be monitored using ME with combined conductivity and
7
8 amperometric detection.³⁸ In addition to these methods, there are several reports of ME
9
10 coupled to electrochemical or conductivity detection for determination of nitrite and
11
12
13
14
15 nitrate.³⁹⁻⁴¹
16

17
18 As described above, the most common method for the quantitation of NO has been
19
20 capillary or microchip electrophoresis through the detection of its metabolites, nitrite and
21
22
23
24
25
26
27
28
29
30
31
32
33
34
35
36
37
38
39
40
41
42
43
44
45
46
47
48
49
50
51
52
53
54
55
56
57
58
59
60

As described above, the most common method for the quantitation of NO has been capillary or microchip electrophoresis through the detection of its metabolites, nitrite and nitrate, or by reacting NO with a fluorescent probe. In this report, a method that allows the direct detection of NO and its metabolites simultaneously in macrophage cells using ME-EC is described. The electrophoretic method permits subminute separation of NO, nitrite, and cellular antioxidants as well as potential interferences and other electrochemically active intracellular components (e.g., tyrosine and nitrotyrosine). This approach makes it possible to gather information regarding the overall redox status of the macrophage cells along with NO production. The method was used to investigate NO and intracellular GSH levels in macrophages under native and stimulated conditions. The ME-EC method reported here will be adapted in the future for single cell analysis studies.

2. Materials and Methods

2.1. Materials and Reagents

The following chemicals and materials were used as received: SU-8 10 photoresist and SU-8 developer (MicroChem Corp., Newton, MA, USA); AZ 1518 photoresist and 300 MIF developer (Mays Chemical Co., Indianapolis, IN, USA); photolithography film

1
2
3 mask (50,000 dpi; Infinite Graphics Inc., Minneapolis, MN, USA); N(100) 100 mm (4")
4
5 silicon (Si) wafers (Silicon, Inc., Boise, ID, USA); chrome and AZ1518 positive
6
7 photoresist coated soda lime glass substrate (4" × 4" × 0.090", Nanofilm, Westlake, CA,
8
9 USA); Pt film-coated glass substrates (2000 Å Pt layer over 200 Å Ti) (The Stanford
10
11 Nanofabrication Facility, Stanford, CA, USA); Sylgard 184 Silicone Elastomer Kit:
12
13 Polydimethylsiloxane (Ellsworth Adhesives, Germantown, WI, USA); Titanium (Ti)
14
15 etchant (TFTN; Transene Co., Danvers, MA, USA); epoxy and 22 gauge Cu wire
16
17 (Westlake Hardware, Lawrence, KS, USA); silver colloidal paste (Ted Pella, Inc.,
18
19 Redding, CA, USA); acetone, 2-propanol (isopropyl alcohol, IPA), 30% H₂O₂, H₂SO₄,
20
21 HNO₃, NaOH, HCl, and Trypan blue (Fisher Scientific, Fair Lawn, NJ, USA); sodium
22
23 nitrite, boric acid, tetradecyltrimethylammonium bromide (TTAB),
24
25 tetradecyltrimethylammonium chloride (TTAC), ascorbic acid (AA), tyrosine, reduced
26
27 glutathione, sodium azide, potassium iodide, NaCl, Lipopolysaccharides from
28
29 Escherichia coli 0111:B4, and Griess reagent (modified) (Sigma, St. Louis, MO, USA)
30
31 and buffered oxide etchant (JT Baker, Austin, TX, USA). All water used was ultrapure
32
33 (18.3 MΩ·cm) (Milli-Q Synthesis A10, Millipore, Burlington, MA, USA).
34
35
36
37
38
39
40

41 **2.2. PDMS Fabrication**

42
43 The fabrication of PDMS-based microfluidic devices has been described
44
45 previously.⁴² Briefly, SU-8 10 negative photoresist (for electrophoresis channels) was
46
47 spin-coated on a 4 in diameter Si wafer to a thickness of 15 ± 1 μm using a Cee 100
48
49 spincoater (Brewer Science Inc., Rolla, MO, USA). The wafer was then transferred to a
50
51 programmable hotplate (Thermo Scientific, Asheville, NC, USA) for a soft bake at 65°C
52
53 for 2 min and then 95°C for 5 min. Microfluidic channel designs were created using
54
55
56
57
58
59
60

1
2
3 AutoCad LT 2004 (Autodesk, Inc., San Rafael, CA, USA) and printed onto a
4 transparency film at a resolution of 50,000 dpi (Infinite Graphics Inc., Minneapolis, MN,
5 USA). The coated wafer was covered with the transparency film mask and exposed
6 (344 mJ/cm² using an i-line UV flood source (ABM Inc., San Jose, CA, USA)).
7
8 Following the UV exposure, the wafer was post-baked at 65°C for 2 min and 95°C for 10
9 min. The wafer was then developed in SU-8 developer, rinsed with IPA, and dried
10 under nitrogen. A final “hard-bake” was performed at 175°C for 2 h. The thickness of the
11 raised photoresist, which corresponds to the depth of the PDMS channels, was
12 measured with a profilometer (Alpha Step-200, Tencor Instruments, Mountain View, CA,
13 USA). PDMS microstructures were made by casting a 10:1 mixture of PDMS elastomer
14 and curing agent, respectively, against the patterned Si master. A simple-T device
15 containing a 5 cm separation channel (from the T intersection to the end of the
16 separation channel) and 0.75 cm side arms was used for these studies. The width and
17 depth of the electrophoresis microchannels were 40 μm and 14 μm, respectively. Holes
18 for the reservoirs were created in the polymer using a 4 mm biopsy punch (Harris Uni-
19 core, Ted Pella Inc., Redding, CA, USA).

2.3. Platinum Electrode Fabrication

20 All electrochemical measurements were obtained using 15 μm Pt working
21 electrodes. Electrodes were either fabricated using an in-house magnetron sputtering
22 system (AXXIS DC magnetron sputtering system, Kurt J. Lesker Co., Jefferson Hills,
23 PA, USA) or received from the Stanford nanofabrication facility. Details of fabrication of
24 Pt electrodes provided by the Stanford nanofabrication facility were reported
25 previously.⁴³ In the Stanford plates, the Pt electrodes are deposited on top of the glass
26
27
28
29
30
31
32
33
34
35
36
37
38
39
40
41
42
43
44
45
46
47
48
49
50
51
52
53
54
55
56
57
58
59
60

1
2
3 surface. To obtain better stability, Pt electrodes were fabricated in-house by making a
4
5 500–600 nm trench in the glass substrate using a procedure previously reported by our
6
7 group.⁴⁴ Briefly, the electrode designs were created using AutoCad LT 2004 (Autodesk,
8
9 San Rafael, CA, USA) and printed onto a transparency film at a resolution of 50,000 dpi
10
11 (Infinite Graphics, Minneapolis MN, USA). Then the electrode design was patterned on
12
13 a chrome and AZ1518 positive photoresist-coated soda lime glass plate. The plate was
14
15 developed using an AZ[®]300 MIF (Capitol Scientific, Inc., Austin, TX, USA) solution for
16
17 30 s and then baked at 100°C for 10 min on a programmable hotplate (Thermo
18
19 Scientific, Asheville, NC, USA). Once the photoresist layer was developed, the exposed
20
21 chrome layer was the shape of the electrode. This chrome layer was then etched using
22
23 chrome etchant to expose the glass surface underneath. Next, the glass plate was
24
25 etched for about 5 min using a 10:1 buffered oxide etchant (JT Baker, Austin, TX, USA)
26
27 to obtain a 500 to 600 nm trench. It has been observed that if the trench is not deep
28
29 enough (below 400 nm), the Pt-deposited electrodes are not stable under high applied
30
31 potentials (greater than 1200 mV) and the Pt electrode flakes off the trench during
32
33 electrophoresis. The plate was washed thoroughly with CaCO₃ and water after buffered
34
35 oxide etching, and the depth of the trench was measured using an Alpha-step 200
36
37 profilometer (Tencor Instruments). The plate was dried at 100°C for 10 min and then
38
39 exposed to an oxygen plasma for 1 min (March Plasmod, Concord, CA, USA). The
40
41 glass plate was immediately transferred to an AXXIS DC magnetron sputtering system
42
43 (Kurt J. Lesker Co.). After pumping down the vacuum chamber of the sputtering system
44
45 to a pressure of 1.0×10^{-6} Torr, a 20-nm Ti layer was deposited (220 V deposition
46
47 voltage, 40 s deposition time, and 5.0×10^{-3} Torr deposition pressure) and then a Pt
48
49
50
51
52
53
54
55
56
57
58
59
60

1
2
3 layer was deposited (200 V deposition voltage, 17 to 20 min deposition time, and $5.0 \times$
4
5 10^{-3} Torr deposition pressure). After metal deposition, the glass plate was washed with
6
7 acetone to remove the photoresist layer along with all excess Pt. The remaining chrome
8
9 was then removed from the plate with chrome etchant. The width and height of the
10
11 resulting Pt electrodes were measured again using an Alpha-step 200 profilometer.
12
13

14 15 **2.4. Solution Preparation**

16
17 All solutions were made using 18.3 M Ω ultrapure water from a Millipore A10
18
19 system. Stock solutions of nitrite (NO_2^- , 10 mM), hydrogen peroxide (H_2O_2 , 10 mM),
20
21 GSH (10 mM), KI (5 mM), NaN_3 (5 mM), and AA (10mM) were all prepared in ultrapure
22
23 water using appropriate amounts and were stored at 4°C. To dissolve tyrosine (Tyr, 10
24
25 mM), the solution was acidified using 1–1.5 M HCl. Subsequent dilutions of each stock
26
27 solution for use in the microchip system were made in the appropriate run buffer at the
28
29 time of analysis. For separation and sampling buffer, a boric acid (20 mM) stock solution
30
31 was prepared and the pH was adjusted to 11 using 10 M or 1 M NaOH solution. The
32
33 pH-adjusted boric acid buffer was diluted with other buffer constituents in order to obtain
34
35 a 10 mM boric acid solution. The buffer pH was measured after dilution and before
36
37 adding surfactant. The buffer pH was 10.3–10.7. TTAC (100 mM) stock solution, NaCl
38
39 (50 mM) stock solution, and ultrapure water were used for buffer dilution.
40
41
42
43
44
45

46 47 **2.5. Chip Construction and Electrophoresis Procedure**

48
49 PDMS microchips consisting of a simple-T design with a 5 cm separation channel
50
51 were used for all studies. Amperometric signals were recorded using a 15 μm Pt
52
53 working electrode against a Ag/AgCl reference electrode, which was placed in the buffer
54
55 waste reservoir after the separation ground lead (Figure 1A). The chip containing the
56
57
58
59
60

1
2
3 separation channel was aligned and reversibly sealed to the glass plate containing the
4 Pt electrode. For in-channel detection, the electrode was placed exactly at the channel
5
6 end of the separation channel as shown in Figure 1B.
7
8
9

10 Electrophoretic separations were carried out using reverse polarity with TTAC as
11 the cationic surfactant to modify the channel walls. Two negative high voltage Pt leads
12 (Pt wire) were placed in the sample and buffer reservoirs, while two earth ground Pt
13 leads were placed in the sample waste and buffer waste reservoirs. For sampling, -2200
14 V was employed, while -2400 V was used for the separation. A gated injection was used
15 to inject the sample, with an injection time between 0.5 and 1 s. Boric acid buffer
16 conditions were evaluated for the separation of nitrite, azide (interference), iodide,
17 tyrosine, GSH, AA, and H₂O₂. To balance the conductivity difference between the cell
18 lysate and separation buffer, 7.5 to 10 mM NaCl was added to the run buffer. The cells
19 were lysed in buffered solution containing surfactant (10 mM boric acid and 2 mM
20 TTAC) without NaCl.
21
22
23
24
25
26
27
28
29
30
31
32
33
34
35

36 **2.6. Electrochemical Detection**

37
38 EC detection was accomplished using a modified model of an 8151BP, 8100-K6, or
39 9051 single- or dual-channel wireless, electrically isolated potentiostat (Pinnacle
40 Technology Inc., Lawrence, KS, USA) operating in a two-electrode format (Pt working;
41 Ag/AgCl reference: Bioanalytical Systems, West Lafayette, IN, USA). The model 8151P,
42 8100-K6, and 9051 potentiostats have a sampling rate of 5 Hz (Gain = 5,000,000 V/A,
43 Resolution = 30 fA), 10 Hz (Gain = 5,000,000 V/A, Resolution = 27 fA), and 6.5 to 13 Hz
44 (Gain = 5,000,000 V/A, Resolution = 47 fA), respectively. Pinnacle Acquisition
45 Laboratory (PAL or Sirenia) software was used for all data acquisition. The data
46
47
48
49
50
51
52
53
54
55
56
57
58
59
60

1
2
3 acquisition is performed via wireless data transmission or Bluetooth from the
4
5 potentiostat to a computer. A working electrode potential of 1100 mV versus Ag/AgCl
6
7 reference was used for all experiments.
8
9

10 **2.7. Cell Culture and Preparation**

11
12 RAW 264.7 cells were purchased from American Type Culture Collection (ATCC,
13
14 Manassas, VA, USA) and cultured in Dulbecco's Modified Eagle's medium containing
15
16 10% (v/v) fetal bovine serum, L-glutamine (2 mM), penicillin (50 IU/mL), and
17
18 streptomycin (50 µg/mL) (ATCC). The cells were maintained in a humidified
19
20 environment at 37°C and 5% CO₂ and cultured in 25 mL polystyrene culture flasks
21
22 (Fisher Scientific). Cells were passaged every 2–3 days to avoid overgrowth.
23
24
25

26 *Cell Viability*

27
28 Cell viability was measured using the Trypan blue (Fisher Scientific) exclusion
29
30 assay and a hemocytometer cell count (C-Chip disposable hemocytometer, Bulldog Bio,
31
32 Inc., Portsmouth, NH, USA). The RAW cell suspension was diluted using a 1:1 to 1:3
33
34 ratio (based on cell density) with a 0.4% Trypan blue solution. The number of viable
35
36 cells and the cell density were determined using a 4 mm² total area hemocytometer.
37
38 Native RAW cells typically had densities of about 5 million cells in a 25 cm² flask prior to
39
40 passaging.
41
42
43
44

45 *Stimulation Protocol*

46
47 Stimulation of NO production in cells was accomplished using purified LPS from the
48
49 *Escherichia coli* line 0111:B4. A freshly prepared 50 µL aliquot of a 10 µg/mL LPS stock
50
51 solution was added to healthy RAW 264.7 cells in a 25 cm² cell culture flask to obtain a
52
53 100 ng/mL final LPS concentration and then incubated for 24 h. An unstimulated RAW
54
55
56
57
58
59
60

1
2
3 macrophage cell flask from the same population was incubated under identical
4
5 conditions and used as a control (native) for each stimulation experiment.
6
7

8 *Sample Preparation*

9

10 The protocol used for cell analysis is shown in the Figure 2A. Cells were grown in
11
12 25 cm² polystyrene flasks until they reached approximately 80% confluence. At 80%
13
14 confluence level, there are around 5 million RAW cells in the flask. These cells were
15
16 stimulated using LPS and, after the stimulation period (24 h with a 100 ng/mL final LPS
17
18 concentration, Figure 2B), cells were harvested using a scraper and centrifuged at 3500
19
20 rpm for 2.5 min to make a live cell pellet. Before centrifugation, 250 µL of the cell
21
22 solution was taken out for cell counting. The supernatant medium was then removed,
23
24 leaving only the cell pellet. Then the cell pellet was washed with 10 mM phosphate
25
26 buffered saline at pH 7.4. Next the cell pellet was lysed using a lysis buffer containing
27
28 10 mM boric acid and 2 mM TTAC at pH 10.3 to 10.7. Both the high pH and surfactant
29
30 assisted with the immediate lysis of cells. Higher molecular weight compounds such as
31
32 proteins and cell membranes were removed by centrifugation of the lysate for 2–7 min
33
34 using a 3 kDa molecular weight cut-off filter (VWR International, West Chester, PA,
35
36 USA). The filtered lysate was then loaded into the sample reservoir of the microchip.
37
38
39
40
41
42

43 For the standard addition studies, four 25 cm² cell flasks with the same passage
44
45 number were harvested and lysed using 1 mL of 10 mM boric acid with 2 mM TTAC at
46
47 pH 10.3 (for 1 cell flask, 250 µl of buffer was used). The lysate was divided into five
48
49 portions, and the internal standard was appropriately added to ensure a final
50
51 concentration 10 µM. Standard addition concentrations of 15, 30, 60, and 120 µM nitrite
52
53 were chosen and the required nitrite volume from a 1 mM nitrite standard was added to
54
55
56
57
58
59
60

1
2
3 the cell lysates. Before the addition of iodide and nitrite, an equal volume of solution
4
5 was removed from the cell lysate.
6
7

8 *Griess Assay Protocol*

9
10 The Griess assay was performed using 96-well plates and a plate reader (Molecular
11 Devices, Spectra Max M5, Sunnyvale, CA, USA). To perform the assay, 100 μL of the
12 filtered cell lysate was added into 100 μL of Griess reagent, left to react for 15 min, after
13
14 which the absorbance at 540 nm was recorded using the plate reader. A buffer
15
16 background was always employed for these measurements. For nitrite quantitation, a
17
18 calibration curve was prepared using nitrite standards from 1 to 50 μM . Cell counts were
19
20 taken before lysing the cells, and the final nitrite concentration was calculated, taking
21
22 into account the cell counts.
23
24
25
26
27

28 **3. Results and Discussion**

29 **3.1. Microchip Electrophoresis with Electrochemical Detection**

30
31 There are two primary electrode configurations that are used for ME under reverse
32
33 polarity conditions. The electrode can be placed either slightly inside the channel (in-
34
35 channel) or outside the channel (end-channel). The advantage of the in-channel
36
37 configuration is it allows higher resolution between closely migrating species, which
38
39 cannot be separated by end-channel configuration due to band broadening.⁴³ Therefore,
40
41 faster separations and shorter analysis times can be obtained using the in-channel
42
43 configuration. Also, we have observed an increase in peak height, better sensitivity, and
44
45 a higher number of theoretical plates with the in-channel configuration compared to the
46
47 end-channel configuration.⁴³ However, an important consideration with in-channel
48
49 detection is that one must take into account the working electrode potential shift that
50
51
52
53
54
55
56
57
58
59
60

1
2
3 occurs due to the separation voltage when an electrode is placed inside the channel. To
4
5 minimize this effect in these experiments, the working electrode was placed exactly at
6
7 the channel end, which still preserves the higher resolution and separation efficiencies
8
9 characteristic of in-channel detection that are necessary for these studies, but
10
11 minimizes the potential shift at the working electrode (Figure 1B).⁴³
12
13
14

15 **3.2. Separation Buffer Optimization**

16
17 The analytes of interest in our studies of nitrosative stress included NO, nitrite (a
18
19 metabolite of NO), GSH (cellular antioxidant), AA (cellular antioxidant), and tyrosine
20
21 (amino acid, which is nitrated in the presence of ONOO⁻). We have previously reported
22
23 the separation and detection of several of these analytes (nitrite, ascorbic acid, tyrosine,
24
25 glutathione, and H₂O₂) by ME-EC as compounds that could potentially interfere with the
26
27 quantitation of NO and nitrite in macrophage cell lysates.⁴³ For the macrophage cell
28
29 lysate studies described here, the same separation conditions (10 mM boric acid with 2
30
31 mM TTAB) with slight modifications were utilized.
32
33
34
35

36 *Internal Standard, Surfactant, and Interferences*

37
38 To quantitate the compounds in the cell lysates and increase the precision of the
39
40 analytical method, iodide was incorporated as an internal standard and, therefore, had
41
42 to be taken into consideration during the separation optimization procedures. In our
43
44 previous studies, TTAB was used to reverse the EOF. In these studies, TTAB was
45
46 replaced with TTAC, where the counter ion is Cl⁻ instead of Br⁻. It was found that
47
48 bromide can be oxidized to Br₂ at around 1200 mV versus Ag/AgCl, leading to an
49
50 increase in background current at the EC detector. Bromide, chloride, and nitrite have
51
52 similar electrophoretic mobilities and, hence, migrate closely. We observed a vacancy
53
54
55
56
57
58
59
60

1
2
3 peak close to the nitrite peak during initial cell studies due to high Cl^- content. Another
4 species that needed to be separated from the cell lysate components was azide. The
5 molecular weight cut-off filters used for cell lysate filtration were found to contain a small
6 amount of this compound, which is used as an anti-microbial agent. Under these
7 separation conditions, azide migrated between nitrite and iodide but did not interfere
8 with either measurement.
9

17 *Conductivity Issues*

20 During the initial analysis of the cell lysates, it was observed that the sampling
21 current was always higher than the separation current and the high conductivity
22 samples suppressed the nitrite peak due to destacking.⁴⁵ A similar suppression in the
23 nitrite signal has been reported in CE when a high conductivity sample was analyzed.²²
24 To reduce the amount of salt and matrix components present in biological samples prior
25 to CE analysis, solid-phase microextraction,²⁴ acetonitrile addition (acetonitrile lowers
26 the sample conductivity),²² dialysis,⁴⁶ and pre-electrophoresis separation⁴⁷ have been
27 widely employed.
28
29

32 An alternative approach to avoid nitrite destacking is to increase the conductivity of
33 the separation buffer by using sodium chloride. Figure 3A shows the nitrite peak
34 suppression that occurs when standards are prepared in a high conductivity buffer (10
35 mM boric acid with 2 mM TTAC and 10 mM NaCl at pH 10.3) and the separation buffer
36 consists of a low conducting buffer (10 mM boric acid with 2 mM TTAC at pH 10.3). In
37 contrast, Figure 3B illustrates that the addition of 7.5 mM NaCl to the separation buffer
38 causes an approximately 3-fold increase in the nitrite signal. This can then be compared
39 to a case where both the sample buffer and separation buffer are low conductivity
40
41
42
43
44
45
46
47
48
49
50
51
52
53
54
55
56
57
58
59
60

1
2
3 buffers (10 mM boric acid with 2 mM TTAC at pH 10.3) (Figure 3C). In this last case, the
4
5 nitrite signal is similar to that seen in Figure 3B. These experiments confirmed the
6
7 destacking of nitrite in high conductivity samples. All three electropherograms used for
8
9 the comparison studies were recorded with the same microchip, working electrode, and
10
11 working electrode potential.
12
13

14 **3.3. Detection of Nitrite from Macrophage Cell Lysates**

15
16 RAW 264.7 macrophage cells are known to produce large amounts of NO through
17
18 the activation of iNOS. LPS, an endotoxin in negative gram bacteria and an external
19
20 stimulant, can be used to activate iNOS.^{48, 49} It has been reported that RAW 264.7
21
22 macrophage cells produce significantly higher amounts of NO in the presence of LPS.^{48,}
23
24
25
26
27
28
29
30
31
32
33
34
35
36
37
38
39
40
41
42
43
44
45
46
47
48
49
50
51
52
53
54
55
56
57
58
59
60

49 In these studies, a LPS concentration of 100 ng/mL over 24 h was used for cell stimulation (Figure 2A). A substantial difference in physical appearance between native and LPS-stimulated cells was observed, as can be seen in Figure 2B.

To compare intracellular nitrite produced in stimulated and native macrophage cells, bulk cell lysates were prepared as shown in Figure 2A, and analyzed by ME-EC. The Griess assay was also performed to compare with the results obtained with ME-EC. To confirm that NO production was due solely to an increase in iNOS activity, a separate set of cells was exposed to L-NAME, which is a known inhibitor of iNOS, before LPS stimulation and analyzed via Griess assay. These results were compared to those from native and LPS-stimulated cell lysate samples with the same passage number. Each flask contained around 5 million cells, which were lysed in 250 μ L of borate buffer (10 mM boric acid with 2 mM TTAC at pH 10.3 to 10.7) in order to minimize the sample conductivity (Figure 3A).

1
2
3
4
5
6
7
8
9
10
11
12
13
14
15
16
17
18
19
20
21
22
23
24
25
26
27
28
29
30
31
32
33
34
35
36
37
38
39
40
41
42
43
44
45
46
47
48
49
50
51
52
53
54
55
56
57
58
59
60

Figure 4A shows the electropherograms obtained for native and LPS-stimulated cell lysates using our ME-EC device. The migration times for the first two peaks in the native cell electropherogram were similar to those for nitrite and iodide standards, and the peak identities were confirmed by spiking with standards. Azide was also spiked to further ensure that the nitrite peak does not comigrate with azide during cell studies.

3.4. Comparison of Nitrite Production in Macrophage Cell Lysates using ME-EC and Griess Assay

Three different pairs of native and LPS-stimulated cell lysates were analyzed by ME-EC and the Griess assay, respectively, for the comparison of nitrite concentrations. Both methods were used to determine nitrite production increase in LPS-stimulated cells versus native cells (Figure 4B). A t-test was performed to compare the two sets of data (Griess versus ME-EC), and it was found that these two series exhibited no statistical difference at a 90% confidence level. This shows that the nitrite level detected with ME-EC is similar to that seen in the results of the Griess assay.

The nitrite concentration varied from one sample to another due to the samples having different cell counts. Therefore, the cell counts were taken into account in both the Griess assay and ME-EC studies when calculating the final nitrite concentrations. The nitrite production in a single cell was estimated by assuming that the volume of a macrophage is approximately 0.5 pL. The Griess assay results show that the average intracellular concentrations of nitrite in single unstimulated and LPS-stimulated macrophage cells are 0.63 ± 0.16 mM (0.31 ± 0.08 fmol/cell) and 1.69 ± 1.06 mM (0.84 ± 0.53 fmol/cell), respectively.

1
2
3
4
5
6
7
8
9
10
11
12
13
14
15
16
17
18
19
20
21
22
23
24
25
26
27
28
29
30
31
32
33
34
35
36
37
38
39
40
41
42
43
44
45
46
47
48
49
50
51
52
53
54
55
56
57
58
59
60

In the case of ME-EC analysis, an external calibration curve could not be used for the quantitation of nitrite due to the nitrite peak suppression. Therefore, the method of standard additions was used, employing iodide as an internal standard. Two different ME-EC setups were used for the analysis of these samples, and two standard addition calibration curves of the nitrite/iodide response vs. standard addition concentration were plotted. These plots yielded R^2 values of 0.987 and 0.973 resulting in values for intracellular nitrite of 0.58 and 0.83 fmol/cell, respectively. This resulted in an average estimated intracellular nitrite concentration for a single native macrophage cell of 1.41 mM. The average nitrite level in single LPS-stimulated cells was then estimated using the nitrite production increase in LPS-stimulated cells relative to that in native cells, which is a 2.83-fold increase (Figure 4B). Consequently, LPS-stimulated cells have a nitrite concentration of approximately 4.00 mM (1.99 fmol/cell). Goto *et al.* reported similar levels for extracellular nitrite production (1 fmol/cell) in single LPS-stimulated macrophage cells using the Griess reagent and a microfluidic device.³¹

3.5. Direct Detection of NO and Other Electroactive Species in Macrophage Cells

NO Detection

The reason for employing ME-EC in these studies is the ability to directly detect NO, its metabolite NO_2^- , and other cellular electroactive species (e.g., cellular antioxidants) simultaneously. The overall goal is to implement this in a single cell analysis system in the future. Detection of all these species cannot be achieved with the Griess assay or LIF detection alone.

When detecting NO in cell lysates, sample preparation steps were shortened to minimize NO degradation and evaporation. Cells were quickly lysed (10–20 s), and the

1
2
3 lysate was centrifuged for only 2 min. Figure 5 shows electropherograms obtained for
4
5
6 native and LPS-stimulated cell lysates following this procedure. It can be seen that the
7
8 height of the peak that migrates at approximately 30 s decreases over time compared to
9
10 the internal standard peak. The migration time of the decreasing peak is close to the
11
12 neutral marker (32.3 ± 2.1 s), and the quick disappearance of this peak over several
13
14 injections suggests that the compound is unstable. Since cells produce NO following
15
16 LPS stimulation due to the induction of iNOS, this peak is most likely NO. The
17
18 disappearance of this peak is probably due to loss of the gas through the open
19
20 reservoirs on the microchip or permeation through the PDMS. Nitrite was also detected
21
22 during these studies, but the nitrite peak is very small compared to the NO peak (Figure
23
24 5 inset), which confirms that NO disappears from the wells quickly before degradation
25
26 occurs. When the sample preparation time was lengthened, this peak disappeared.
27
28
29
30
31

32 We previously reported a ME method for the detection of NO generated using
33
34 diethylamine NONOate (DEA/NO) and proline NONOate (PROLI/NO) salts.³⁵ The
35
36 migration time of NO in those studies is comparable to the migration time of the
37
38 decaying peak in the cell lysates considering the slight variation in chip-to-chip migration
39
40 times that is expected in PDMS-based systems.³⁵ It can be seen in the native cell
41
42 lysate that the last peak does not decay at the same rate as the unstable NO peak seen
43
44 in LPS-stimulated cell lysate. This indicates that the peak observed in the native cell
45
46 sample is contaminated with a more stable electroactive species. This species was
47
48 found to be an interfering filter component that migrates close to the neutral marker
49
50 (Figure 5). Therefore, the NO peak observed in these studies is contaminated.
51
52
53
54
55
56
57
58
59
60

1
2
3
4
5
6
7
8
9
10
11
12
13
14
15
16
17
18
19
20
21
22
23
24
25
26
27
28
29
30
31
32
33
34
35
36
37
38
39
40
41
42
43
44
45
46
47
48
49
50
51
52
53
54
55
56
57
58
59
60

Currently, the NO peak cannot be used for a quantitative comparison of native and stimulated cells due to the necessity for further peak identification, experimental variability, the presence of an interference due to the filters, and, most importantly, the fact that the peak decreases quickly over time due to evaporation and degradation. However, detection of NO will be better accomplished using a single cell analysis microfluidic device where cells are lysed inside the device and the content is immediately analyzed. Since the cell lysis procedure is automated, a single cell cytometric device would provide better precision. Furthermore, a single cell cytometric device eliminates the cell lysate filtering step.

Comparison of Glutathione Levels in Native and Stimulated Cells

Other electroactive species such as tyrosine and GSH were also detected in macrophage cell lysates. However, electropherograms of native and LPS-stimulated cell lysates showed a very small peak or no peak for AA, which agreed with previous ME-LIF studies.³⁶ Macrophages do not naturally produce AA and an AA free media was used for cell culture. Previous studies reported undetectable levels of AA in RAW macrophage cells.⁵⁰

The relative GSH and nitrite levels for three separate LPS-stimulated cell lysates were compared to that of a native cell lysate with the same passage number using the same ME-EC conditions used for nitrite detection. As before, it was found that the nitrite level in LPS-stimulated cells was increased 5.74 ± 2.44 times relative to the native cell lysates. However, the GSH levels showed no significant change (1.30 ± 0.31) when the cells were stimulated with LPS (Figure 6). Hothersall *et al.* also observed that GSH levels were not changed when macrophage cells were stimulated with LPS alone.

1
2
3 However, they have shown that the GSH level changed when the cells were stimulated
4 with LPS and interferon gamma.⁵¹
5
6
7

8 **Conclusion**

9
10 In this paper, a ME-EC method was optimized for the detection of nitrite, NO, and
11 other electroactive species within macrophage cell lysates. ME-EC makes it possible to
12 obtain more information regarding the overall cellular redox state of the cell. It also
13 provides a separation of interfering species from the analytes of interest that cannot be
14 achieved using classical methods such as the Griess assay and fluorescence imaging.
15 Initially, NO production was detected through the detection of nitrite using a ME-EC
16 device. The results obtained for nitrite production between LPS-stimulated and native
17 cell lysates using ME-EC were compared to those from the Griess assay. Then this
18 method was used for the direct detection of NO and other electroactive species in the
19 cell lysate. An unstable species, which had many of the chemical and physical
20 properties of NO, was detected during these studies. However, the NO peak cannot
21 currently be used for a quantitative comparison of native and stimulated cells. The
22 detection of NO will be better accomplished using a single cell analysis microfluidic
23 device where cells are lysed inside the device and the content immediately analyzed.
24 We have already reported a single cell chemical cytometric device for NO detection
25 from Jurkat cells using a NO-selective fluorophore.²⁹ The ultimate goal is to use ME-EC
26 to measure multiple redox-active species in a single cell as an indication of nitrosative
27 stress.
28
29
30
31
32
33
34
35
36
37
38
39
40
41
42
43
44
45
46
47
48
49
50
51
52
53
54
55
56
57
58
59
60

Acknowledgements

This research was funded by the following NIH grants: R01NS042929 and R21 NS061202 and COBRE grant P20GM103638. The authors thank Pinnacle Technologies, Inc., Lawrence, KS, USA for the development and loan of the isolated potentiostats. M.K.H. was a recipient of an American Heart Association postdoctoral fellowship. G.C. was supported by the International Internship Program, University of Catania, Italy. J.M.S. has received support from the Madison and Lila Self Graduate Fellowship, University of Kansas, Lawrence, KS, USA. The authors would also like to thank Prof. José Alberto Fracassi da Silva, Pann Pichetsurnthorn, Keelan Trull, Diogenes Meneses do Santos, and Emilie R. Mainz for assistance with some of the experiments; Prof. Christian Schöneich for helpful discussions; Ryan Grigsby for help with microchip fabrication; and Nancy Harmony for editorial support.

Figure Captions

Figure 1. (A) Schematic of ME-EC setup with in-channel configuration. (B) Electrode alignment

Figure 2. (A) Diagram of the stimulation and sample preparation protocol for RAW 264.7 macrophage cells prior to ME-EC and Griess assay analyses. (B) Images of RAW 264.7 macrophage cells after 24 h without stimulation (left) and with LPS stimulation (right).

Figure 3. Electropherograms of a standard containing 100 μM nitrite, 10 μM iodide (internal standard), 50 μM tyrosine, and 200 μM hydrogen peroxide (neutral marker) using a 10 mM boric acid and 2 mM TTAC buffer at pH 10.3 while varying the sample and run buffer conductivities. (A) High conductivity sample buffer (10 mM NaCl) and normal separation buffer. (B) High conductivity sample buffer (10 mM NaCl) and high conductivity separation buffer (7.5 mM NaCl). (C) No change to the conductivity of the sample and separation buffer.

Figure 4. (A) Comparison of LPS-stimulated (top) and native (bottom) RAW 264.7 macrophage cell lysates using ME-EC. (B) Comparison of the ME-EC method and the Griess assay for determining the increase in nitrite concentration resulting from a 24 h LPS stimulation relative to the nitrite concentration produced from native cells. The sample was prepared in 10 mM boric acid and 2 mM TTAC buffer at pH 10.3 and the separation was achieved with a 10 mM boric acid, 7.5 mM NaCl and 2 mM TTAC buffer at pH 10.3.

Figure 5. Detection of NO in cell lysate. LPS-stimulated cell lysate (top) and native cell lysate (bottom). Inset is a magnified portion of the LPS-stimulated cell lysate. The sample was prepared in 10 mM boric acid and 2 mM TTAC buffer at pH 10.3 and the

1
2
3 separation was achieved with a 10 mM boric acid, 7.5 mM NaCl and 2 mM TTAC buffer
4
5 at pH 10.3.
6
7

8 Figure 6. Comparison of the nitrite and glutathione (GSH) levels as a result of LPS
9
10 stimulation relative to that of the native cell lysate. The sample was prepared in 10 mM
11
12 boric acid and 2 mM TTAC buffer at pH 10.3 and the separation was achieved with a 10
13
14 mM boric acid, 10 mM NaCl and 2 mM TTAC buffer at pH 10.7.
15
16
17
18
19
20
21
22
23
24
25
26
27
28
29
30
31
32
33
34
35
36
37
38
39
40
41
42
43
44
45
46
47
48
49
50
51
52
53
54
55
56
57
58
59
60

References

1. P. Pacher, J. S. Beckman and L. Liaudet, *Physiol. Rev.*, 2007, **87**, 315-424.
2. J. MacMicking, Q. Xie and C. Nathan, *Annu. Rev. Immunol.*, 1997, **15**, 323-350.
3. V. Calabrese, C. Cornelius, E. Rizzarelli, J. B. Owen, A. T. Dinkova-Kostova and D. A. Butterfield, *Antioxid. Redox Signal.*, 2009, **11**, 2717-2739.
4. K. D. Kröncke, K. Fehsel and V. Kolb-Bachofen, *Nitric Oxide*, 1997, **1**, 107-120.
5. M. N. Moller, Q. Li, J. R. Lancaster, Jr. and A. Denicola, *IUBMB Life*, 2007, **59**, 243-248.
6. F. O. Martinez, L. Helming and S. Gordon, *Annu. Rev. Immunol.*, 2009, **27**, 451-483.
7. S. Gordon and P. R. Taylor, *Nat. Rev. Immunol.*, 2005, **5**, 953-964.
8. L. S. Lilly, in *Pathophysiology of Heart Disease : A Collaborative Project of Medical Students and Faculty*, Lippincott Williams & Wilkins, Baltimore, MD, 5th edn., 2011.
9. L. Minghetti and G. Levi, *Prog. Neurobiol.*, 1998, **54**, 99-125.
10. M. Valko, D. Leibfritz, J. Moncol, M. T. D. Cronin, M. Mazur and J. Telser, *Int. J. Biochem. Cell Biol.*, 2006, **39**, 44-84.
11. H. Zhang and H. J. Forman, *Semin. Cell Dev. Biol.*, 2012, **23**, 722-728.
12. J. B. Schulz, J. Lindenau, J. Seyfried and J. Dichgans, *Eur. J. Biochem.*, 2000, **267**, 4904-4911.
13. C. Amatore, S. Arbault and A. C. W. Koh, *Anal. Chem.*, 2010, **82**, 1411-1419.
14. D. Tsikas, *J. Chromatogr. B*, 2007, **851**, 51-70.
15. D. Tsikas, *Anal. Biochem.*, 2008, **379**, 139-163.
16. F. Bedioui and S. Griveau, *Electroanal.*, 2013, **25**, 587-600.
17. E. M. Hetrick and M. H. Schoenfish, *Annu. Rev. Anal. Chem.*, 2009, **2**, 409-433.
18. R. Trouillon, *Biol. Chem.*, 2013, **394**, 17-33.
19. A. Gomes, E. Fernandes and J. L. F. C. Lima, *J. Fluoresc.*, 2006, **16**, 119-139.
20. X. Zhang, W. S. Kim, N. Hatcher, K. Potgieter, L. L. Moroz, R. Gillette and J. V. Sweedler, *J. Biol. Chem.*, 2002, **277**, 48472-48478.
21. X. Ye, S. S. Rubakhin and J. V. Sweedler, *Analyst*, 2008, **133**, 423-433.
22. M. A. Friedberg, M. E. Hinsdale and Z. K. Shihabi, *J. Chromatogr. A*, 1997, **781**, 491-496.
23. E. Morcos and N. P. Wiklund, *Methods Mol. Biol.*, 2004, **279**, 21-34.
24. D. Y. Boudko, *Methods Mol. Biol.*, 2004, **279**, 9-19.
25. D. Y. Boudko, B. Y. Cooper, W. R. Harvey and L. L. Moroz, *J. Chromatogr. B*, 2002, **774**, 97-104.
26. W. S. Kim, X. Ye, S. S. Rubakhin and J. V. Sweedler, *Anal. Chem.*, 2006, **78**, 1859-1865.
27. K. Govindaraju, M. Toporsian, M. E. Ward, D. K. Lloyd, E. A. Cowley and D. H. Eidelman, *J. Chromatogr. B*, 2001, **762**, 147-154.
28. R. A. Hunter, B. J. Privett, W. H. Henley, E. R. Breed, Z. Liang, R. Mittal, B. P. Yoseph, J. E. McDunn, E. M. Burd, C. M. Coopersmith, J. M. Ramsey and M. H. Schoenfish, *Anal. Chem.*, 2013, **85**, 6066-6072.
29. E. C. Metto, K. Evans, P. Barney, A. H. Culbertson, D. B. Gunasekara, G. Caruso, M. K. Hulvey, J. A. Fracassi da Silva, S. M. Lunte and C. T. Culbertson, *Anal. Chem.*, 2013, **85**, 10188-10195.
30. P. A. Vogel, S. T. Halpin, R. S. Martin and D. M. Spence, *Anal. Chem.*, 2011, **83**, 4296-4301.
31. M. Goto, K. Sato, A. Murakami, M. Tokeshi and T. Kitamori, *Anal. Chem.*, 2005, **77**, 2125-2131.
32. M. K. Hulvey and R. S. Martin, *Anal. Bioanal. Chem.*, 2009, **393**, 599-605.
33. S. T. Halpin and D. M. Spence, *Anal. Chem.*, 2010, **82**, 7492-7497.

- 1
2
3 34. S. Letourneau, L. Hernandez, A. N. Faris and D. M. Spence, *Anal. Bioanal. Chem.*,
4 2010, **397**, 3369-3375.
5 35. D. B. Gunasekara, M. K. Hulvey, S. M. Lunte and J. A. Fracassi da Silva, *Anal. Bioanal.*
6 *Chem.*, 2012, **403**, 2377-2384.
7 36. E. R. Mainz, D. B. Gunasekara, G. Caruso, D. T. Jensen, M. K. Hulvey, J. A. Fracassi da
8 Silva, E. C. Metto, A. H. Culbertson, C. T. Culbertson and S. M. Lunte, *Anal. Methods*,
9 2012, **4**, 414-420.
10 37. R. Kikura-Hanajiri, R. S. Martin and S. M. Lunte, *Anal. Chem.*, 2002, **74**, 6370-6377.
11 38. M. Vázquez, C. Frankenfeld, W. K. T. Coltro, E. Carrilho, D. Diamond and S. M. Lunte,
12 *Analyst*, 2010, **135**, 96-103.
13 39. M. J. A. Shiddiky, K. S. Lee, J. Son, D. S. Park and Y. B. Shim, *J. Agric. Food Chem.*,
14 2009, **57**, 4051-4057.
15 40. P. Troška, R. Chudoba, L. Danč, R. Bodor, M. Horčíciak, E. Tesařová and M. Masár, *J.*
16 *Chromatogr. B*, 2013, **930**, 41-47.
17 41. S. D. Noblitt, F. M. Schwandner, S. V. Hering, J. L. Collett, Jr. and C. S. Henry, *J.*
18 *Chromatogr. A*, 2009, **1216**, 1503-1510.
19 42. M. K. Hulvey, C. N. Frankenfeld and S. M. Lunte, *Anal. Chem.*, 2010, **82**, 1608-1611.
20 43. D. B. Gunasekara, M. K. Hulvey and S. M. Lunte, *Electrophoresis*, 2011, **32**, 832-837.
21 44. D. E. Scott, R. J. Grigsby and S. M. Lunte, *ChemPhysChem*, 2013, **14**, 2288-2294.
22 45. J. Boden and K. Bächmann, *J. Chromatogr. A*, 1996, **734**, 319-330.
23 46. P. R. Haddad, P. Doble and M. Macka, *J Chromatogr A*, 1999, **856**, 145-177.
24 47. A. R. Timerbaev, K. Fukushi, T. Miyado, N. Ishio, K. Saito and S. Motomizu, *J.*
25 *Chromatogr. A*, 2000, **888**, 309-319.
26 48. R. B. Lorschach, W. J. Murphy, C. J. Lowenstein, S. H. Snyder and S. W. Russell, *J. Biol.*
27 *Chem.*, 1993, **268**, 1908-1913.
28 49. T. K. Held, X. Weihua, L. Yuan, D. V. Kalvakolanu and A. S. Cross, *Infect. Immun.*,
29 1999, **67**, 206-212.
30 50. C.-D. Badrakhan, F. Petrat, M. Holzhauser, A. Fuchs, E. E. Lomonosova, G. H. de and
31 M. Kirsch, *J. Biochem. Biophys. Methods*, 2004, **58**, 207-218.
32 51. J. S. Hothersall, F. Q. Cunha, G. H. Neild and A. A. Norohna-Dutra, *Biochem. J.*, 1997,
33 **322**, 477-481.
34
35
36
37
38
39
40
41
42
43
44
45
46
47
48
49
50
51
52
53
54
55
56
57
58
59
60

Figure 1

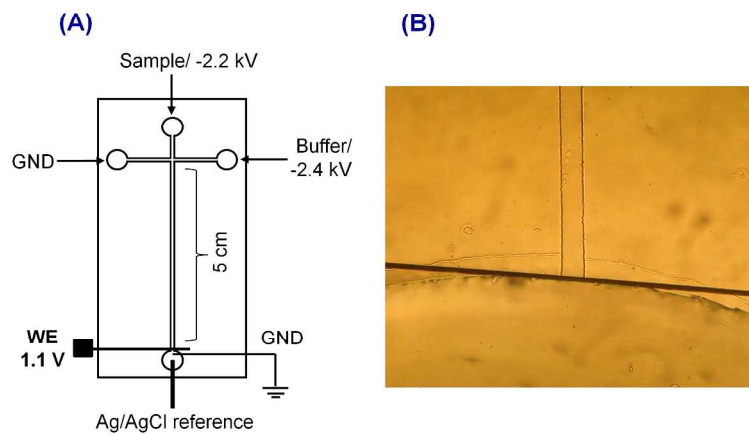


Figure 1. (A) Schematic of ME-EC setup with in-channel configuration. (B) Electrode alignment
254x190mm (300 x 300 DPI)

Figure 2

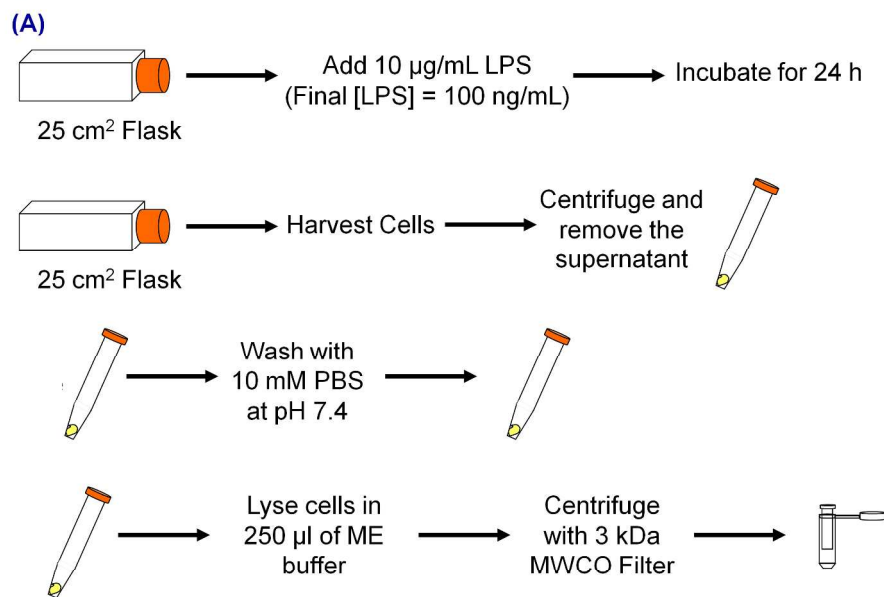
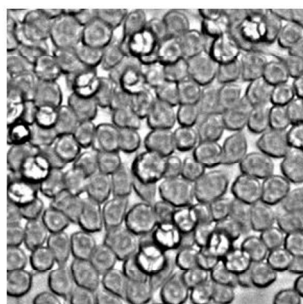
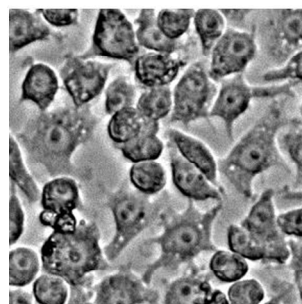


Figure 2. (A) Diagram of the stimulation and sample preparation protocol for RAW 264.7 macrophage cells prior to ME-EC and Griess assay analyses.
254x190mm (300 x 300 DPI)

(B)



Native macrophages
after 24 h



100 ng/mL LPS-stimulated
macrophages after 24 h

Figure 2. (B) Images of RAW 264.7 macrophage cells after 24 h without stimulation (left) and with LPS stimulation (right).
254x190mm (300 x 300 DPI)

Figure 3

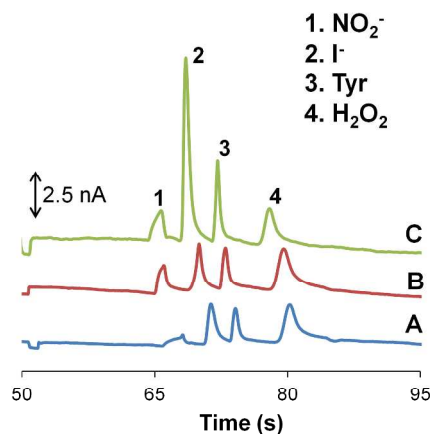


Figure 3. Electropherograms of a standard containing 100 μM nitrite, 10 μM iodide (internal standard), 50 μM tyrosine, and 200 μM hydrogen peroxide (neutral marker) using a 10 mM boric acid and 2 mM TTAC buffer at pH 10.3 while varying the sample and run buffer conductivities. (A) High conductivity sample buffer (10 mM NaCl) and normal separation buffer. (B) High conductivity sample buffer (10 mM NaCl) and high conductivity separation buffer (7.5 mM NaCl). (C) No change to the conductivity of the sample and separation buffer.

254x190mm (300 x 300 DPI)

Figure 4

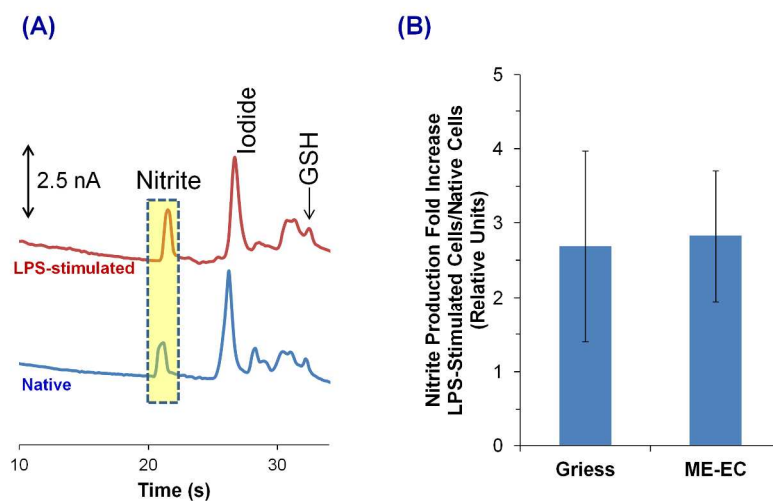


Figure 4. (A) Comparison of LPS-stimulated (top) and native (bottom) RAW 264.7 macrophage cell lysates using ME-EC. (B) Comparison of the ME-EC method and the Griess assay for determining the increase in nitrite concentration resulting from a 24 h LPS stimulation relative to the nitrite concentration produced from native cells. The sample was prepared in 10 mM boric acid and 2 mM TTAC buffer at pH 10.3 and the separation was achieved with a 10 mM boric acid, 7.5 mM NaCl and 2 mM TTAC buffer at pH 10.3.
254x190mm (300 x 300 DPI)

Figure 5

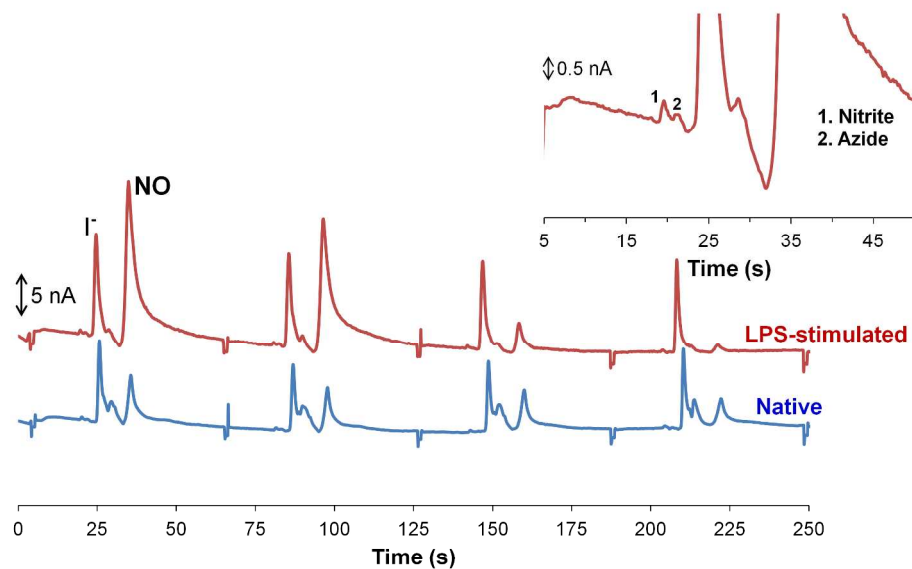


Figure 5. Detection of NO in cell lysate. LPS-stimulated cell lysate (top) and native cell lysate (bottom). Inset is a magnified portion of the LPS-stimulated cell lysate. The sample was prepared in 10 mM boric acid and 2 mM TTAC buffer at pH 10.3 and the separation was achieved with a 10 mM boric acid, 7.5 mM NaCl and 2 mM TTAC buffer at pH 10.3.
254x190mm (300 x 300 DPI)

Figure 6

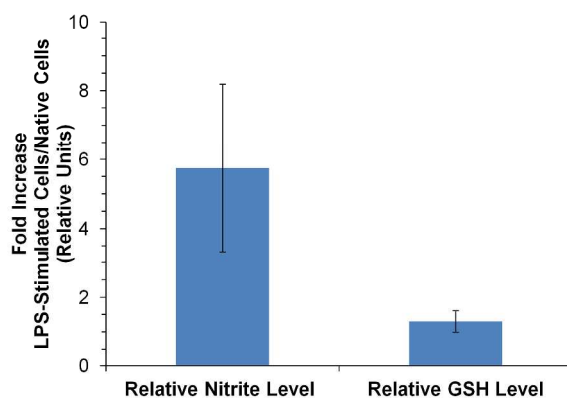
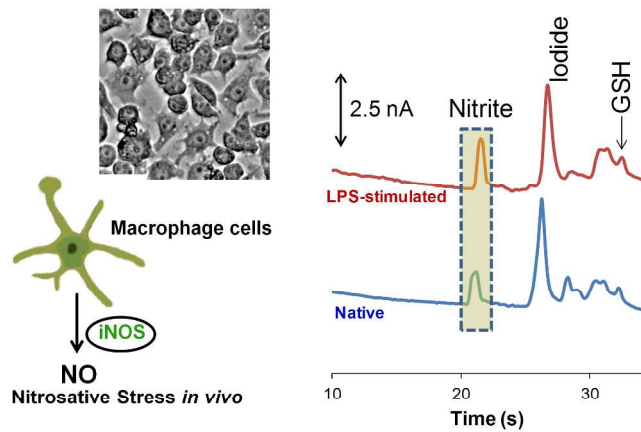


Figure 6. Comparison of the nitrite and glutathione (GSH) levels as a result of LPS stimulation relative to that of the native cell lysate. The sample was prepared in 10 mM boric acid and 2 mM TTAC buffer at pH 10.3 and the separation was achieved with a 10 mM boric acid, 10 mM NaCl and 2 mM TTAC buffer at pH 10.7.

254x190mm (300 x 300 DPI)

1
2
3
4
5
6
7
8
9
10
11
12
13
14
15
16
17
18
19
20
21
22
23
24
25
26
27
28
29
30
31
32
33
34
35
36
37
38
39
40
41
42
43
44
45
46
47
48
49
50
51
52
53
54
55
56
57
58
59
60



254x190mm (300 x 300 DPI)